

Laser-induced resonant transition at 470.724 nm in the $v = n - l - 1 = 2$ cascade of metastable antiprotonic helium atoms

F. E. Maas, R. S. Hayano, T. Ishikawa, H. Tamura, and H. A. Torii
Department of Physics, University of Tokyo, 7-3-1 Hongo, Bunkyo-ku, Tokyo 113, Japan

N. Morita
Institute for Molecular Science, Myodaiji, Okazaki 444, Japan

T. Yamazaki, I. Sugai, and K. Nakayoshi
Institute for Nuclear Study, University of Tokyo, 3-2-1 Midori-cho, Tanashi, Tokyo 188, Japan

F. J. Hartmann, H. Daniel, T. von Egidy, B. Ketzer, A. Niestroj, S. Schmid, and W. Schmid
Physik Department, Technische Universität München, D-85747 Garching, Germany

D. Horváth
Central Research Institute for Physics, Research Institute for Particle and Nuclear Physics, H-1525 Budapest, Hungary

J. Eades and E. Widmann
CERN, CH-1211 Geneva 23, Switzerland
 (Received 17 April 1995)

A laser-induced resonant transition in metastable antiprotonic helium atoms has been found at a wavelength of 470.724 ± 0.002 nm and assigned to the transition $(n, l) = (37, 34) \rightarrow (36, 33)$. From the time evolution of the laser resonance intensity, the decay rate of the $(37, 34)$ state was determined to be $1.17 \pm 0.09 \mu\text{s}^{-1}$, about 60% larger than the theoretical radiative decay rate. The sum of the initial populations in the $v = n - l - 1 = 2$ decay chain was $23 \pm 4\%$ of the total number of metastable atoms formed.

PACS number(s): 36.10.Gv

In 1991 an unusual longevity of antiprotons stopping in liquid helium was observed at KEK [1]. Since then this phenomenon has been investigated extensively using the Low Energy Antiproton Ring (LEAR) at CERN [2–5]. These experiments indicated that the long-lived antiprotons are those trapped in metastable states of neutral $\bar{p}e^{-}\text{He}^{2+}$ ($\equiv \bar{p}\text{He}^{+}$) atoms with large principal quantum numbers (n) and orbital angular momenta (l), both $\sim \sqrt{M/m} = 38$, as first suggested in [6,7]. More recently laser resonance spectroscopy has been used to study metastable atoms [8,9]. The last metastable state in each metastable cascade that is characterized by $v = n - l - 1$ (radial node number) can be resonantly de-excited to a lower Auger dominated short-lived state [10,11], resulting in a sharp peak in the \bar{p} annihilation time spectrum at the laser ignition time. This technique resulted in our discovery of a resonance line at 597.259 nm [8], which we assigned to $(n, l) = (39, 35) \rightarrow (38, 34)$ at the end point of the $v = 3$ metastable cascade. However, this accounted for only $(11 \pm 2)\%$ of the metastable atoms formed. In the present paper, we report the discovery of a transition at the end of the $v = 2$ radiative cascade that accounts for a further $(23 \pm 4)\%$ of the initial population of metastable atoms.

We used the same arrangement as for the previous experiment [8,9]. Antiprotons from LEAR at an intensity of about $2 \times 10^4 \bar{p}/\text{s}$ and a momentum of 200 MeV/c were stopped in cold helium gas ($T = 5.5$ K, $p = 600$ mbar). The time difference t was recorded between the entry of each \bar{p} into our helium gas target and the detection of its delayed annihila-

tion products. We used two independent pulsed dye-laser systems. These were triggered only when metastable $\bar{p}\text{He}^{+}$ had been formed in our helium target by the \bar{p} (i.e., only when it had still not annihilated 70 ns after its entry into the target). The delay time between the laser light and the \bar{p} arrival was reduced to 1.35 μs in the present experiment. The wavelength of the $(n, l) = (37, 34) \rightarrow (36, 33)$ transition was, according to several theoretical predictions, expected to be around 471 nm, and this region was scanned by changing the laser wavelength step by step. Figure 1(a) shows an annihilation time spectrum when the light from one laser pulse, arriving 1.35 μs after the \bar{p} arrival, was tuned to a wavelength of 470.724 nm.

The resonance peak in Fig. 1(a) is much more intense than the previously reported 597.259-nm $v = 3$ transition [8]. Consequently, there is a distinct depletion in the annihilation time spectrum immediately after the peak. The peak profile shows an exponential decay with a time constant of 16.6 ± 0.1 ns. This value represents an upper bound for the Auger lifetime of the $(36, 33)$ level since dephasing collisions in the gas slow down the deexcitation from the $(37, 34)$ level.

The resonance line shape was measured by scanning the wavelength. To check the reproducibility and the possible existence of systematic changes of the resonance line we scanned over the resonance four times. The background subtracted counts in the peak divided by the total number of delayed annihilations is shown in Fig. 1(b) as a function of the laser wavelength for one of the scans. The solid line in Fig. 1(b) shows the results of a fit to the experimental data of

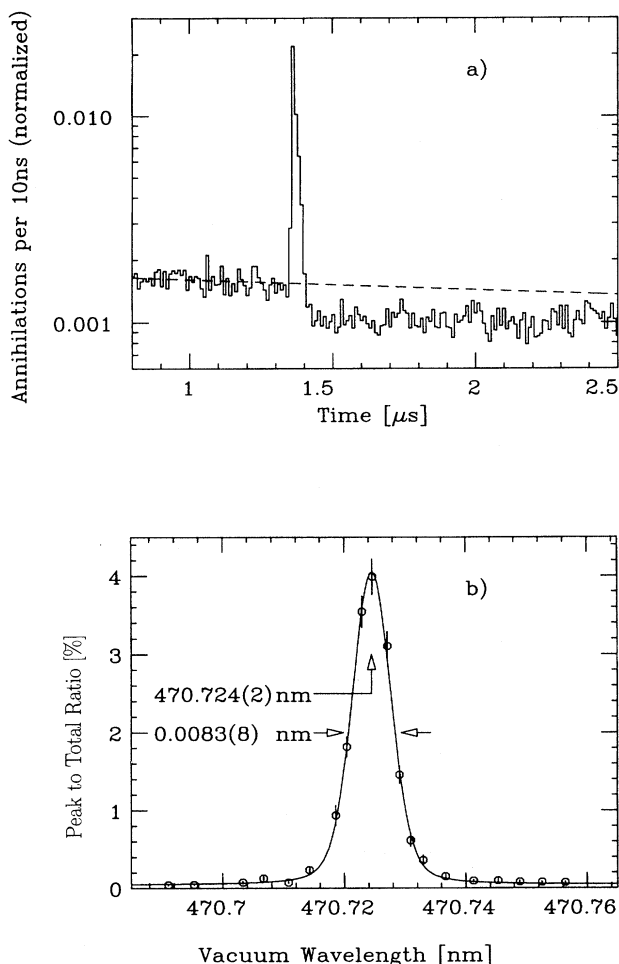


FIG. 1. (a) Normalized delayed annihilation time spectrum when the wavelength of the laser pulse was tuned to 470.724 nm at $t_1 \sim 1.35 \mu\text{s}$. Resonant “depopulation” at this wavelength results in a distinct change in the annihilation time spectrum, producing a sharp peak followed immediately by a corresponding depletion. The signal peak profile shows an exponential decay with a time constant of $16.6 \pm 0.1 \text{ ns}$. (b) Resonance intensity as a function of the laser wavelength. The solid line represents a fit of the Lorentzian profile convoluted with a Gaussian to the data points.

a Lorentzian line shape convoluted with a Gaussian. The fitted central frequency is $470.7245 \pm 0.0001 \text{ nm}$ and the full width at half maximum of the resonance is $0.0083 \pm 0.0008 \text{ nm}$. By far the largest contribution to the linewidth is the saturation broadening due to the high laser power employed. Calibration of the laser wavelength against suitable standard absorption lines in argon gives a correction of $-0.6 \pm 1.5 \text{ pm}$, resulting in a value for the transition wavelength of $470.724 \pm 0.002 \text{ nm}$. Our present experimental accuracy of 4 ppm in the determination of the transition wavelength is dominated by the frequency standard employed and is much larger than the statistical error of 0.2 ppm. A reduction of the error by at least one order of magnitude seems to be possible in the near future.

The experimental transition wavelength is compared with the theoretical values in Fig. 2. The agreement between the

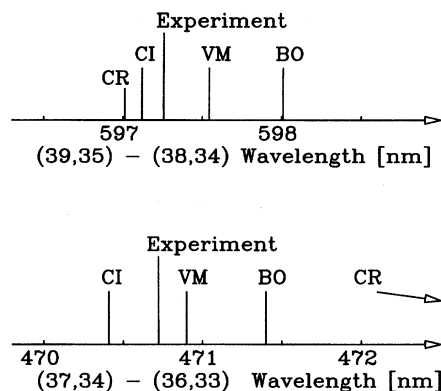


FIG. 2. Various theoretical predictions on the transition wavelength (BO, CI, VM, and CR; see the text for explanations) are compared with the experimental values for the two laser resonance transitions found in the previous and present experiments.

experiment and the predicted theoretical values is at present at the 0.6% level. The value from atomic configuration-interaction calculations (CI) is 470.4 nm [12]. The molecular model with the Born-Oppenheimer approximation (BO) gives a value of 471.4 nm [13,14]. More recent calculations using the large configuration-space variational method (VM) yield 470.9 nm [15], and nonadiabatic coupled rearrangement channel variational calculations (CR) give 473.5 nm [16].

To determine the decay rate and population of the relevant states in the $v=2$ cascade, we used the same method as for the $v=3$ decay chain [9]: we measured the change in the laser resonance intensity as a function of the time of arrival (t_1) of the laser light. The measured resonance intensity at t_1 normalized to the total number of delayed annihilations [$I_1(t_1)$] is directly proportional to the population of the (37,34) state, denoted by $N_{37}(t_1)$. The state depopulation efficiency ϵ is then the ratio $I_1(t_1)/N_{37}(t_1)$. If we could depopulate the (37,34) state completely, ϵ would be 1. In addition, the resonance intensity of a second laser pulse $I_2(t_1, t_2)$ normalized to the total delayed annihilations at laser ignition times $t_2 > t_1$ reveals the feeding of the depleted state from states above it. We therefore study the cascade by mapping $I_1(t_1)$ and $I_2(t_1, t_2)$.

The experimental data for $I_1(t_1)$ and $I_2(t_1, t_2)$ are shown in Fig. 3. For the single-laser series, t_1 values between 1.6 μs and 6.9 μs were chosen. In the double-laser series, t_1 was fixed at 2.4 μs , 3.4 μs , and 4.4 μs while $t_2 - t_1$ was varied from 0.2 μs to 5.2 μs . The small ratio of $I_2(t_1, t_2)/I_1(t_1)$ for times $t_2 \sim t_1$ shows that the depopulation efficiency ϵ is large whereas the steep rise of $I_2(t_1, t_2)$ with t_2 indicates fast refilling from the upper states.

There is a $\Delta n = \Delta l = 1$ propensity rule for the radiative transitions [12,13], implying that $N_{37}(t)$ mainly reflects the populations and lifetimes in the $\rightarrow(39,36) \rightarrow (38,35) \rightarrow (37,34)$ radiative transition ladder. For a quantitative analysis of the laser delay measurements we employed three simplified models in which we assume that only the two, three, or four lowest metastable states in the ladder are initially populated, all radiative transitions with $\Delta v \neq 0$ being neglected.

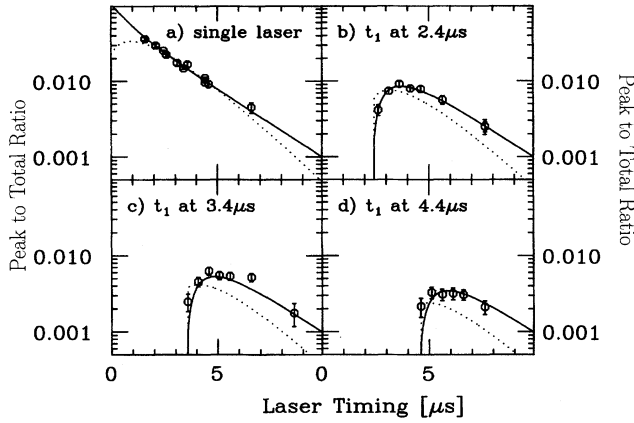


FIG. 3. Time evolution of the resonance intensity measured with the laser tuned to 470.724 nm using (a) a single light pulse; (b) two light pulses, the first at 2.4 μs ; (c) two light pulses, the first at 3.4 μs ; and (d) two light pulses, the first at 4.4 μs . The solid line shows a representative fit result employing the two-level model, which is almost indistinguishable from the three- and four-level model results. Any fitted function with λ_{37} fixed to the theoretical radiative rate (dotted curve) deviates significantly from the experimental data.

The corresponding set of differential equations describing the time evolution of $N_n(t)$ in the $\nu=2$ decay led to analytical functions for the measured values of $I_1(t_1)$ and $I_2(t_1, t_2)$, which were fitted in a simultaneous least-squares method to the experimental data, with the $N_n(0)$ (initial population), λ_n (decay rate), and ϵ as fit parameters.

Prior to the analysis of the experimental data for $I_1(t_1)$ and $I_2(t_1, t_2)$ we tested systematically the sensitivity of the method by simulating $I_1(t_1)$ and $I_2(t_1, t_2)$ for various values of the populations and decay rates. We found that we could reproduce the total initial population [the sum of all $N_n(0)$] as well as the decay rate of the lowest level (λ_{37}) independently of the model employed. However, concerning the population of the upper levels [$N_{38}(0)$ and higher], the method gives rather the sum of the populations and does not allow a determination of the population and decay rates of the individual states.

An overview of the results of the analysis of the experimental data is given in Table I. A two-level model fits the experimental data best, yielding λ_{37} and the total initial population. Here $N_{38}(0)$ and λ_{38} represent the accumulation of higher state population, which is reflected in the unrealistic (slower than the radiative rate) value for λ_{38} . The three-level results are similar to the two-level results, but λ_{38} and λ_{39} are fixed to the theoretical radiative rates. From the experimental data, we find a total $\nu=2$ fraction at the instant of formation ($t=0$) of $(23\pm 4)\%$ of all metastable atoms. Common to all fit results and independently of the assumed model is the fact that some 80% of the population in the $\nu=2$ transition chain is concentrated on the (37,34) and (38,35) states. We should stress that the region below $t=1.35 \mu\text{s}$ is still inaccessible to our laser probe in the present experiment. Consequently, the $t=0$ populations of Table I have been obtained by fitting the data from later times and might not correspond to the true values.

TABLE I. Typical sets of $N_n(0)$ (percent of total delayed), λ_n (in μs^{-1}), and ϵ from fitting to the experimental $I_1(t_1)$ and $I_2(t_1, t_2)$ data. In the last column the calculated radiative rates that include sidefeeding are given. The asterisk denotes a fixed value.

Parameter	Two-level fit	Three-level fit	Calc. rates
$N_{37}(0)$	11 ± 2	16 ± 2	
$N_{38}(0)$	12 ± 1	4 ± 2	
$N_{39}(0)$		6 ± 1	
$N_{\text{all}}(0)$	23 ± 2	25 ± 3	
λ_{37}	1.17 ± 0.06	1.16 ± 0.05	0.73
λ_{38}	0.42 ± 0.06	0.67*	0.67
λ_{39}		0.60*	0.60
ϵ	0.93 ± 0.03	0.93 ± 0.03	
Reduced χ^2	1.7	1.9	

Together with the previously reported population in the $\nu=3$ decay chain of $(11\pm 2)\%$ [9], we have up to now accounted for $(34\pm 4)\%$ of the total delayed annihilation population. The remaining 66% are expected to be in the $\nu=1$ and $\nu=0$ cascades. The extracted decay rate ($1.17\pm 0.09 \mu\text{s}^{-1}$) of the (37,34) state was found to be consistent with the decay constant of a “depletion” spectrum (difference of time spectra on resonance and off resonance) and is about 60% larger than the theoretical radiative decay rate of $0.73 \mu\text{s}^{-1}$ [12,13]. On the other hand, from our previous measurement of the time evolution of the resonance intensity, the decay rate of the (39,35) state was determined to be $0.72\pm 0.02 \mu\text{s}^{-1}$, which was in good agreement with theoretical calculations of the radiative rate when these include correlation between the \bar{p} and the e^- [12,13]. This suggests that for the present (37,34) state there may be considerable competition from Auger transitions whose partial rate amounts to some $0.44\pm 0.09 \mu\text{s}^{-1}$. On the other hand, the experimental data indicate that the upper level decay rates ($\lambda_{38}, \lambda_{39}, \lambda_{40}$) are not faster than the theoretical radiative decay rates.

The observation of this resonance line, together with evidence for feeding from higher states, has unambiguously established the formation of metastable antiprotonic helium atoms $\bar{p}\text{He}^+$ as the source of the observed longevity of the \bar{p} . In the near future, we hope to resolve the fine and hyperfine structure of our $\bar{p}\text{He}^+$ atom. In conjunction with more exact calculations now being made by our theoretical colleagues, such experiments can open the way to high-precision measurements of the fundamental properties of the antiproton, just as muonium [17,18] and positronium [19] have led to improved understanding of the muon and the positron.

We are indebted to the LEAR and PS staff at CERN for their tireless dedication to providing us with the antiproton beam and to P. Greenland, Y. Kino, O. Kartavtsev, K. Ohtsuki, and I. Shimamura for making their theoretical results available to us. The present work is supported by the Grants-in-Aid for Specially Promoted Research and for International Scientific Research of the Japanese Ministry of Education, Science and Culture and the Japan Society for the Promotion of Science. F.E.M. acknowledges financial support from INOUE.

- [1] M. Iwasaki, S. N. Nakamura, K. Shigaki, Y. Shimizu, H. Tamura, T. Ishikawa, R. S. Hayano, E. Takada, E. Widmann, H. Ota, M. Aoki, P. Kitching, and T. Yamazaki, *Phys. Rev. Lett.* **67**, 1246 (1991).
- [2] T. Yamazaki, E. Widmann, R. S. Hayano, M. Iwasaki, S. N. Nakamura, K. Shigaki, F. J. Hartmann, H. Daniel, T. von Egidy, P. Hofmann, Y.-S. Kim, and J. Eades, *Nature* **361**, 238 (1993).
- [3] S. N. Nakamura, R. S. Hayano, M. Iwasaki, K. Shigaki, E. Widmann, T. Yamazaki, H. Daniel, T. von Egidy, F. J. Hartmann, P. Hofmann, Y.-S. Kim, and J. Eades, *Phys. Rev. A* **49**, 4457 (1994).
- [4] E. Widmann, H. Daniel, J. Eades, T. von Egidy, F. J. Hartmann, R. S. Hayano, W. Higemoto, J. Hoffmann, T. M. Ito, Y. Ito, M. Iwasaki, A. Kawachi, N. Morita, S. N. Nakamura, N. Nishida, W. Schmid, I. Sugai, H. Tamura, and T. Yamazaki, *Nucl. Phys. A* **558**, 679c (1993).
- [5] E. Widmann, I. Sugai, T. Yamazaki, R. S. Hayano, M. Iwasaki, S. N. Nakamura, H. Tamura, T. M. Ito, A. Kawachi, N. Nishida, W. Higemoto, Y. Ito, N. Morita, F. J. Hartmann, H. Daniel, T. von Egidy, W. Schmid, J. Hoffmann, and J. Eades, *Phys. Rev. A* **51**, 2870 (1995).
- [6] G. T. Condo, *Phys. Lett.* **9**, 65 (1964).
- [7] J. E. Russell, *Phys. Rev. Lett.* **23**, 63 (1969); *Phys. Rev.* **188**, 187 (1969); *Phys. Rev. A* **1**, 721 (1970); **1**, 735 (1970); **1**, 742 (1970).
- [8] N. Morita, M. Kumakura, T. Yamazaki, E. Widmann, H. Masuda, I. Sugai, R. S. Hayano, F. E. Maas, H. A. Torii, F. J. Hartmann, H. Daniel, T. von Egidy, B. Ketzer, W. Müller, W. Schmid, D. Horvath, and J. Eades, *Phys. Rev. Lett.* **72**, 1180 (1994).
- [9] R. S. Hayano, F. E. Maas, H. A. Torii, N. Morita, M. Kumakura, T. Yamazaki, H. Masuda, I. Sugai, F. J. Hartmann, H. Daniel, T. von Egidy, B. Ketzer, W. Müller, W. Schmid, D. Horvath, J. Eades, and E. Widmann, *Phys. Rev. Lett.* **73**, 1485 (1994); **73**, 3181(E) (1994).
- [10] N. Morita, K. Ohtsuki, and T. Yamazaki, *Nucl. Instrum. Methods Phys. Res. Sect. A* **330**, 439 (1993).
- [11] K. Ohtsuki (private communication).
- [12] T. Yamazaki and K. Ohtsuki, *Phys. Rev. A* **45**, 7782 (1992).
- [13] I. Shimamura, *Phys. Rev. A* **46**, 3776 (1992); and private communication.
- [14] P. T. Greenland and R. Thürwächter, *Hyperfine Interact.* **76**, 355 (1993); P.T. Greenland (private communication).
- [15] O. I. Kartavtsev, in *Proceedings of the Third Biennial Conference on Low-energy Antiproton Physics (LEAP94)*, Bled, Slovenia, 1994 (World Scientific, Singapore, in press).
- [16] Y. Kino (private communication).
- [17] F. G. Mariam *et al.*, *Phys. Rev. Lett.* **49**, 993 (1982).
- [18] F. E. Maas, B. Braun, H. Geerds, K. Jungmann, B. E. Matthias, G. zu Putnitz, I. Reinhard, W. Schwarz, L. Willmann, and L. Zhang, *Phys. Lett. A* **187**, 247 (1994).
- [19] M. S. Fee *et al.*, *Phys. Rev. A* **48**, 192 (1993).